

Adaptive RBF with hyperparameter optimisation for aeroacoustic applications

International Journal of Aeroacoustics
2022, Vol. 21(1-2) 22–42

© The Author(s) 2022

Article reuse guidelines:

sagepub.com/journals-permissions

DOI: 10.1177/1475472X221079545

journals.sagepub.com/home/jae



Lorenzo Burghignoli , **Monica Rossetti**, **Francesco Centracchio**,
Giorgio Palma  and **Umberto Iemma**

Abstract

The present work reports an investigation on the use of adaptive metamodels based on radial basis functions (RBFs) for aeroacoustic applications of highly innovative configurations. The relevance of the topic lies on the paramount importance of metamodeling techniques within the design optimisation process of disruptive aircraft layouts. Indeed, the air traffic growth, consequently the hard environmental constraints imposed by regulations, will make a technological breakthrough, an imperative need within few years. As a consequence, the engineering community is paying particular attention to the development of innovative techniques for the design of unconventional configurations. For this class of applications, the designer cannot successfully rely on historical data or low-fidelity models, and the expensive direct simulations remain the only valuable design strategy. In this regard, it can be demonstrated that the use of surrogate models, *i.e.*, metamodels, significantly reduces the computing costs, especially in view of a robust approach to the optimised design. In order to further improve the efficiency of metamodel-based techniques, dynamic approaches based on hyperparameter optimisation and adaptive sampling procedures have been recently developed. The case study presented here pertains the exploiting of dynamic RBF-based metamodels for noise shielding applications. The analysis of the metamodel performances and its convergence properties shows how the final number of direct simulations is significantly reduced by the hyperparameter optimisation algorithm, still strongly depending on the choice of the RBF kernel function.

Keywords

Simulation-based design, aircraft noise, metamodeling, radial basis functions, aeroacoustics

Date received: 20 April 2021; revised: 11 August 2021; accepted: 2 October 2021

Department of Engineering, Roma Tre University, Roma, Italy

Corresponding author:

Lorenzo Burghignoli, Department of Engineering, Roma Tre University, Via Vito Volterra 62, Roma 00146, Italy.

Email: lorenzo.burghignoli@uniroma3.it

Introduction

The sustainable development of the airborne transportation system is currently one of the major commitments of the aeronautical engineering community to guarantee the satisfaction of the growing market demand in a context where most of the existing airports are close to the operational saturation. Despite oscillations due to world-wide crises, the aviation industry has constantly grown throughout the last century and is expected to further increase in the near future. The average annual rate of 4.4% in terms of transport capacity (revenue passenger kilometres, RPK) experienced over the period 1989–2009,¹ is foreseen to grow more than 5% in the 2030 horizon.² This growth is mostly due to the progressive access to the civil aviation system of the emerging economies (such as Asia, Middle-East, Africa and Latin America) with more than 6% RPK annual increment during the last decades.^{2,3} A broader ambition of 24/7 operations has been set for air transport as a whole to accommodate mobility needs by 2050, allowing in particular full usage of existing infrastructures in line with the Flightpath 2050 global vision.⁴ In addition to the standard aviation of today, as explained by Rizzi,⁵ Urban Air Mobility is a rapidly emerging market in which new populations will routinely be exposed to aircraft pollution also in urban areas. Although aviation currently accounts for only 2–3% of the 36 billion metric tons of CO_2 emissions of anthropic origin,⁶ these emissions are projected to grow in the foreseeable future as the air traffic increases. The enhancement of the environmental friendliness of commercial aircraft is thus of paramount importance.

Exhaust emissions are not the only problem estimated to be critical. Sustainable development of air traffic implies actions to reduce the noise impact generated by aircraft at airport areas so that the life quality of surrounding communities can be maintained or improved, and the development of new infrastructure is no longer being considered an issue. Indeed, in many places, a negative response to aircraft noise has increased in recent years, having a substantial impact on future extensions of airports which are reaching their capacity limits. The mitigation of aircraft noise levels in areas surrounding airports during the take-off and landing operations is one of the most complex subjects for the aeronautical-community. It requires the involvement of several actors such as airports, local authorities, research organisations, aircraft industry, airlines, regulatory entities and residents (communities living around airports are directly impacted by this aviation noise) for the identification of both noise reduction technologies and strategies such as operational improvements, operating restrictions and land use planning. For this reason, over the last 20 years, the European Union has encouraged and granted a significant number of research projects focused on aircraft noise and chemical pollution reduction. This excellence in noise research and engineering has contributed to the European aircraft industry successes, bringing promising technology concepts to validation and demonstration stages.⁷ The H2020 Work Programme mentions two specific challenges, among others: i) the achievement of the required level of mitigation of noise and adverse health effects in the transport sector and ii) the reinforcement of the competitiveness and performance of EU transport. The high number of world-wide projects currently involved in this research field shows that the recent interest in developing new technologies is not only coming from the industrial sector for commercial and economic purposes, but also from the scientific community as a response to the fast changes the world is experiencing. One of the H2020 framework projects aimed at controlling the aircraft noise is the ANIMA project. The purpose of ANIMA⁸ is to develop innovative methods and suitable tools to mitigate and manage the effects of aircraft noise, improving the quality of life near the airports. The used approach facilitates both the airport growth and the aviation industry's competitiveness, in compliance with the severe environmental constraints. Within ANIMA, seven EREA members (Association of European Research Establishments in Aeronautics), strategic partners, leading universities from all over Europe and major entities of the

European aerospace industry have collaborated to deeply analyse the promising novel concepts and methods which are directly coupled to new low noise and disruptive aircraft configurations desired for the 2035 and 2050 horizons.

So far, a great deal of effort has been accomplished to reduce emissions by applying new technologies to conventional aircraft layouts, such as laminar flow, winglets, improved IC engines, composite materials and active control systems. Even though this effort had helped so far to achieve remarkable improvements, nowadays, an asymptotic limit is being reached in terms of efficiency.⁹ For this reason, new interests have evolved in studying innovative airframe configurations, low-noise technologies based on metamaterials^{10,11} and the use of advanced propulsive systems. During the last decades, ideas about the noise shielding obtained by installing the engines on top of the fuselage have been conceived for both conventional and innovative aircraft configurations. Results of high-level simulations and experimental campaigns have shown the effectiveness of this strategy in terms of noise shielding.^{12,13} For this reason among others, aviation industry has put a great deal of effort into the design of innovative configurations such as the *Blended-Wing-Body*. Studies conducted on this configuration have demonstrated that its large centre body surface shaped as an airfoil contributes to the overall lift force enhancing the aerodynamic efficiency,¹⁴ leads itself excellently to the aforementioned on top engine installation¹⁵ and exploit a greater useful volume compared to that of the standard configurations allowing, in principle, the storage of hybrid-electric propulsion power-plant.^{16,17}

Due to the strong innovation of such concepts, efficient optimisation procedures must be largely employed, since the early stage of the aircraft design, to maximise the aerodynamic and acoustic performances and, at the same time, guarantee constraints to be satisfied. However, the unconventionality of new concepts makes existing semi-empirical and analytical models inapplicable, imposing the inclusion of computationally expensive numerical simulations in the conceptual design frameworks. This fact increases the computational cost of the entire process by order of magnitudes. For example, the estimate of the noise maps on the ground must be done considering all the operations in the time slot of interest, thus imposing the use of simple prediction models, typically based on regression of existing data, to limit the computational cost due to the large number of evaluation points required. Besides, the need to rely on direct numerical methods introduces uncertainties related to both the simulation model accuracy and the unknown operability outside the design point, requiring the use of robust design optimisation,¹⁸ which tremendously increases the computational burden.

Although the computing power is continuously evolving, the complexity of high-fidelity analysis codes, such as finite element analysis, computational fluid dynamics (CFD) and computational aeroacoustics (CAA), still requires a long time to compute. As a consequence, obtaining a very accurate model can sometimes be more costly than the advantages it provides, especially during the conceptual design phase. For these reasons, it is of primary importance the identification of procedures to concentrate the use of the available resources in the exploration of the design space, optimising the extraction of information from the simulations (or experiments). Extensive research has been carried out to overcome the issue of balancing the trade-off between computational efficiency and prediction accuracy.¹⁹ In the development of noise impact management and prediction tools, efficient metamodels can provide an estimate of the effect of unconventional concepts and procedures at a reasonable computational cost.^{20–22}

In the last few decades, adaptive schemes^{23–25} have been conceived to improve the metamodel efficiency in terms of number of points used to obtain the desired accuracy. Following this approach, the training set is not sampled a priori but instead continuously updated during the metamodel construction adding new points where needed.²⁶ In a context of multidisciplinary design

optimisation, a dynamically evolving metamodel can help significantly in reducing the number of calls to the expensive simulation models and avoid the wasting of resources in irrelevant areas of the design space. The development of dynamic metamodels is one of the most promising strategies to answer to the above issues in an effective fashion. Examples of engineering applications of dynamic RBF networks are oriented to the creation of metamodels used in the context of simulation-based design (SBD) optimisation,²⁷⁻²⁹ uncertainty quantification (UQ),³⁰ and reliability analysis (RA).³¹

In the field of surrogate models, the use of radial basis functions (RBFs) for the reproduction of a dataset is a standard, well-established interpolation technique initially introduced by Hardy³² for representing (irregular) topographic surfaces. RBF methods are powerful means to face the problem of reconstructing unknown functions from a set of small data. As it can be found in literature,^{33,34} they are particularly suitable for multivariate functions which are dependent on many variables or parameters, contain non-linearities and are described by (possibly many) scattered data in their domain. RBF models are widely used due to its theoretical simplicity and efficient implementation compared to other techniques such as Kriging, Gaussian Process and Neural Networks.

This work focuses on applying adaptive RBF to build reliable metamodels of aeronautical interest to be embedded in multidisciplinary optimisation processes of unconventional aircraft configurations. Specifically, the aim is to extend the use of dynamic metamodels based on the stochastic RBF formulation introduced in Volpi et al.³⁰ to compare the use of different kernel functions. Indeed, the set of basis functions used for an interpolation problem cannot be fixed in advance, but it should depend on the application case.³⁵

By statistically varying the kernel function hyperparameters, the stochastic RBF approach provides uncertainty quantification to reveal regions of the input space where surrogate predictions are less accurate (i.e. driving further points acquisition to enhance the model actively). As the choice of the kernel hyperparameters strongly depends on the training set properties (number of points and their distributions), an optimisation strategy is included at each iteration of the adaptive scheme to identify suitable values to be used in the stochastic approach.

The paper is organised as follows. The first section is dedicated to the description of the RBF formulations. After a brief description of the standard method, the adaptive formulation based on stochastic RBF is presented. In the next section, the algorithm for the tuning of the hyper parameters and the kernels used in the analyses are introduced. The proposed method is then applied to the case study described in the next section, followed by the presentation of the corresponding results. Finally, the last section collects some concluding remarks.

Standard RBF formulation

The basic idea behind the RBF formulation (Hardy³²) is that we look for a function s that interpolates the data in the points where the target response is known, *i.e.*, it satisfies the conditions $s(x_j) = f_j$, $1 \leq j \leq N$, being x_j the j -th training samples and $f_j = f(x_j)$ the function value. Let's consider a target response $f(\xi)$, solution of a certain problem governed by an arbitrarily complex set of PDEs for $\xi \in D$, where D is the design domain of interest. Also assume that an analytical form of f is not available, and its value can be obtained only numerically through expensive computational tools for specified values of the design variable ξ . Given a training set (TS) of pairs $(\xi_i, f(\xi_i))$ for $i = 1, N_T$, a simple interpolation \tilde{f} of the data using RBF has the form

$$\tilde{f}(\xi) = \sum_{j=1}^{N_T} w_j \varphi(|\xi - \xi_j|) \quad (1)$$

with weights w_j obtained by imposing the values at the TS points and solving the inverse linear problem

$$\mathbf{w} = \mathbf{A}^{-1}\mathbf{f} \quad (2)$$

where $A_{ij} = \varphi(\xi_i, \xi_j)$ and $f_j = f(\xi_j)$.

The condition for the surrogate model to reproduce the training set yields the system of equations for the unknowns w_j . The matrix A is symmetric for sets of distinct data sites and the solution to the fitting problem exists and is unique, if and only if A is non-singular. Therefore, our approximation is the linear combination of shifts of a function, which is radially symmetric with respect to the given norm about their *centres*, or *knots*, where the function is known. In this work, the l_2 norm, *i.e.*, the Euclidean distance, is used for which radial symmetry means that the function value only depends on the Euclidean distance. It can be shown that the distance matrix A based on the Euclidean distance in \mathbb{R}^d is always non-singular for a certain class of basis function.³⁵ Specifically, the scattered data interpolation problem is well-posed under the class of basis functions for which the matrix is positive definite.

Dynamic metamodels based on stochastic RBF

The objective of a dynamic metamodeling approach is not the simple interpolation of data using equation (1) but instead obtaining an optimal training set with the minimum number of points needed to predict the unknown response $f(\xi)$ with the desired accuracy. Therefore, the design space is no longer sampled a priori employing a static design of experiment (DoE) technique but instead dynamically updated where it is more useful, trying to use the minimum number of simulations to represent the function accurately.

In the present section, the dynamic approach based on the stochastic RBF formulation introduced by Volpi et al.³⁰ is described. In this approach, the RBF metamodel is reinterpreted in a statistical fashion introducing a stochastic variation of the RBF kernel hyperparameters. The advantage of a stochastic RBF formulation is the evaluation of the local metamodel uncertainty, which is used to drive the improvement of the TS with new samples in the more uncertain regions. The prediction is made on the so-called validation set, which is an ensemble of points (N_{val}) where the output function is known, left out from the training set to validate the efficiency of the surrogate model.

The surrogate stochastic model for the function $f(\xi)$ is defined considering a stochastic variation of the kernel parameter ε subjected to a probability density function distribution $P(\varepsilon)$. The prediction \hat{f} obtained through the stochastic metamodel is thus defined as the expected value (EV) of the metamodels obtained varying the hyperparameter in the range $[\varepsilon_{min}; \varepsilon_{max}]$

$$\hat{f}(\xi) = EV \left[\sum_{j=1}^{N_T} w_j \varphi(|\xi - \xi_j|, \varepsilon) \right], \varepsilon \in P(\varepsilon) \quad (3)$$

$$= \int_{\varepsilon_{min}}^{\varepsilon_{max}} \hat{f}(\xi, \varepsilon) P(\varepsilon) d\varepsilon \quad (4)$$

Numerically, the EV is calculated through the Monte Carlo method using N_ε points

$$\hat{f}(\xi) = \frac{1}{N_\varepsilon} \sum_{j=1}^{N_\varepsilon} \hat{f}(\xi, \varepsilon_j) \quad (5)$$

The uncertainty is quantified as the difference of the relevant p quantiles of the predictions obtained varying the ε parameter so as to have a 95% confidence band

$$U_{\hat{f}}(\xi) = q(p_1, \xi) - q(p_2, \xi) \quad (6)$$

with $p_1 = 0.975$ and $p_2 = 0.025$. The quantile q , is defined as the inverse function of the cumulative distribution function of the predictions \hat{f} at ξ

$$CDF(y, \xi) = \int_{D_\varepsilon} H\left[y - \hat{f}(\xi, \varepsilon)\right] P(\varepsilon) d\varepsilon \quad (7)$$

where H is the Heaviside step function.

Adopting a dynamic update of the metamodel based on the above mentioned stochastic formulation $\hat{f}_S(\xi)$, at each iteration of the algorithm, the TS is updated with an additional sample located where the metamodel uncertainty is maximum.

The flowchart of the dynamic adaptive algorithm is depicted in Figure 1. Starting from an initial TS , equation (5) is applied to the validation set, and the local value of its uncertainty $U(\xi)$ is calculated. If the maximum value of the uncertainty is above a certain threshold ϵ , the TS is updated by adding a new sample $(\xi, f(\xi))$, which is obtained exploring the variables domain by means of a genetic algorithm.³⁶ Therefore, the objective function for the search algorithm is the maximum uncertainty in prediction of the current surrogate model

$$\xi_{N+1} = \arg \max_D [U(\xi)] \quad (8)$$

It is worth noting that this is the only step where the expensive model is used. Once the point is collected (employing the costly simulation tool), (5) is evaluated and the prediction on the N_{val} points re-computed.

An appropriate choice of the stochastic parameter allows the conjecture that higher values of U correspond to a local lack of knowledge about the target response dynamics. To account, for example, Volpi et al.³⁰ where it is shown the effectiveness of this strategy for a rich set of benchmark functions and a CFD problem for naval applications, polynomial splines are used as kernel functions and the polynomial degree α is used as stochastic parameter, on which a uniform distribution ($P(\alpha) = \text{const}$) in the range $[1, 3]$ is imposed.

The metamodel uncertainty associated with the stochastic variation of the hyperparameters can be used to estimate the region of the domain where the knowledge about the dynamics of the target response needs to be improved. An appropriate selection of the stochastic parameter can link

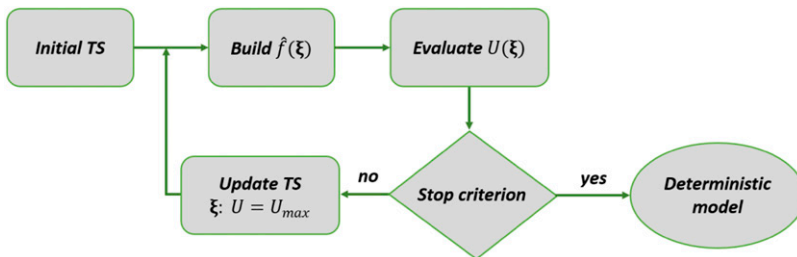


Figure 1. Flowchart of the dynamic adaptive metamodel update.

directly the local statistical dispersion of the metamodel response to the local metamodel accuracy. It is worth noting that this procedure allows for an estimate of the local quality of the surrogate model without additional calls to the expensive simulation models.

The adaptive sampling can follow different approaches depending on the scope of the analysis. In context of uncertainty quantification, a global approximation of the function is required, so the sampling is usually driven by the overall model variance.³⁷ Whereas, for optimisation purpose, the aim is at improving the accuracy of the model in regions of the design space that seems promising, thus focussing on local model improvement. An overview of the most used approaches can be found in.³⁸ For the present application, an approach based on the global metamodel uncertainty is used, as it is done for uncertainty quantification analysis, to explore the entire domain space.

In this work, particular attention is paid to the use of different kernel functions tailored to aeroacoustic applications. To this aim, using the above formulation as a starting point, a tuning strategy is introduced in the adaptive scheme to identify the optimal kernel hyperparameters iteratively.

Hyperparameter tuning

The accuracy of the interpolating function $\tilde{f}(\xi)$ for $\xi \notin TS$ strongly depends on the characteristics of the RBF kernel $\varphi(|\xi - \xi_j|) = \varphi(r)$ and, of course, on the properties of the TS . A condition for the interpolating function to be positive definite and radial for all dimension d is on its monotonicity (completely monotonic and multiply monotone functions),^{33,35} thus on the characteristics of the chosen basis. Indeed, it is important to remember that there is a strong correlation between the shape of the training set (number of points and their distribution) and the distance matrix condition number, so that the well-posedness cannot be ascribed only to the kernel function but to the combination of these factors. Thus, there is a best choice for the kernel hyperparameters that depends on the available training set.

Among the large variety existing in the literature, the analysis is here limited to only a few kernel functions, which are presented in Table 1, having properties of some relevance in the present context.

A relevant taxonomy concerns the oscillatory or non-oscillatory behaviour of the kernel function. This property is of cardinal relevance in the aeroacoustic context, where, as already pointed out, the target response is often a complex wavy field. A further classification can be made in term of properties of the function support: compactly supported functions are identically zero for $r \geq r_0$, whereas not compactly supported functions are defined in the interval $[0, \infty)$. The use of compactly supported functions provides, when properly scaled, banded collocation matrices that have a better behaviour than sparse or dense matrices when centres (*i.e.* TS points) are added *a posteriori*, such as

Table 1. RBF kernels used in the present analysis.

Class	Kernel name	$\varphi(r)$	Hyperparams
Non-oscillatory	Polynomial spline	γr^ϵ	$\gamma; \epsilon$
	Generalised multiquadric	$(1 + \gamma r^2)^\epsilon; \epsilon < 0$	$\gamma; \epsilon$
Oscillatory	Gaussian wave packet	$e^{-(r/\sigma)^2} \cos(\epsilon r)$	$\sigma; \epsilon$
	Truncated Bessel	$\max\left(1 - \frac{ r }{r_0}, 0\right) J_0(\epsilon r)$	$r_0; \epsilon$

in dynamic *TS* definition schemes.³³ This means that, in principle, they are more robust to the training set variation.

The idea to apply oscillatory kernels to aeroacoustic applications comes from recent studies in which these basis functions have been used to approximate numerical solutions for the 2D Helmholtz equation using a radial basis function-generated finite difference scheme (*RBF-FD*) on irregular domains.³⁹⁻⁴² The RBFs are directly used as the basis to approximate the solutions by enforcing the governing equation and boundary conditions on collocation points. The strength of this method for the solution of PDEs lies in the fact that RBFs are a meshless tool so as to not require any prescribed structure (the weights depends only on the distance between the training set points) and they lead to a non-singularity of the interpolation matrix for scattered data in problems with dimensionality $d > 1$. Led by these facts, for the present study, this family of oscillatory kernels has been adopted and compared to more classical kernels to reproduce the dynamics of aeroacoustic engineering problems by interpolating few high-fidelity simulation data.

Many of the kernels used as radial basis function, such as polynomial splines, generalised multiquadrics and Gaussian wave packets, contain a free shape parameter γ that plays a key role in the accuracy of the method. In⁴³ it is shown that the condition number of the system matrix is also influenced by the choice of this parameter. This inter-dependence is known as uncertainty or *trade-off* principle⁴⁴ and is still being investigated. On the other hand, the truncated Bessel does not have a shape parameter but for this kernel we introduce the truncation factor r_0 which makes it compactly supported. Similarly to the shape parameter, the truncation factor is an additional degree of freedom for the metamodel identification and thus it also requires to be carefully selected. In the following, we will refer to both the shape parameter and the truncation factor as the auxiliary hyperparameters to distinguish them from the stochastic hyperparameter ε used in the adaptive scheme.

In their standard formulation, RBF methods involve the solution of linear systems whose matrices are often full and severely ill-conditioned.⁴⁵ Even though several approaches, such as stabilisation techniques, have been applied in literature to overcome the issue of ill-conditioned distance matrix,³⁹ choosing the correct hyperparameters is often the most challenging activity of RBF methods and strongly influences the accuracy of the surrogate model. Many authors dealt with the problem of identifying the best shape parameters for classical kernel functions.⁴⁶⁻⁵² In the present application, we deal with both non-conventional basis functions and adaptive scheme for which the training set is updated throughout the process. For this reasons, the application of empirical formulae cannot be applied directly to the proposed problem. Furthermore, thanks to the development of high computational power, iterative approaches have been formulated to determine the best hyperparameters. Among others, the power-function and the cross-validation methods are the most used. Despite the high computation demand, the method of cross-validation is widely used in the statistics literature. In this method, the optimal hyperparameter values are found minimising a cost function given by the (least-square) error for a sequence of partial fits where a sub-set of centres are left out for the prediction (a series of *test sets* which in batches span all the N_T points).

A special implementation of cross-validation is the leave-one-out cross-validation (LOOCV) where, in round, one point of the training set is left out from the fit until all points are used as test points, which is more robust for small *TS*. Consequently, the evaluation metric is based on the Euclidean norm of the vector $E = E[E_1, \dots, E_N]^T$, where N is the total number of training points available. As it can be observed, this method is even more demanding of the general cross-validation and becomes unfeasible for problems with large sets of data. For this reason, many authors have worked on alternative or simplified algorithm forms to assess and validate the accuracy of their surrogate models. LOOCV forms the basis of the algorithm proposed by Rippa in⁴⁶ for choosing an

optimal value of the shape parameter in the setting of scattered data interpolation with RBFs, requiring less computation effort. While this classical implementation of the leave-one-out algorithm would be rather expensive ($O(N^4)$),³⁵ Rippa showed that the algorithm can be simplified as follows

$$E_{Rippa,i} = \left| f(\xi_i) - \tilde{f}(\xi_i) \right| = \frac{w_i}{A_{ii}^{-1}} \quad (9)$$

where w_i is the i -th coefficient in the interpolant $\tilde{f}(\phi)$ based on all the data points, and A_{ii}^{-1} is the i -th diagonal element of the inverse of the corresponding collocation matrix.⁴⁶ In the case of searching the tuning parameter, the calculation is thus reduced to $O(N^3)$, since the distance matrix is calculated once for each hyperparameter value. Even though this simplification introduces an error, Rippa showed that this error is sufficiently constant over the range of variation, so that the minimum coincides with that obtained using the classical LOOCV approach. For this reason, in the follows this simplified calculation is employed.

Performing hyperparameters tuning means that the model used for the approximation is identified within the analysis process to maximise its fitting capability and accuracy. This strategy can be further applied to the choice of the kernel itself, and often these approaches are coupled.^{53–55}

In the proposed method, a loop on the stochastic (ε) and the auxiliary hyperparameters is added to the process comparing the error norms for different values of the hyperparameters, choosing the optimal ones that yield the minimum error norm. Adding this further step, the adaptive algorithm reported in Figure 1 becomes the one depicted in Figure 2. As said, Rippa's method has been used as metric for the research of optimal hyperparameters. At each iteration of the adaptive scheme, the best hyperparameters for the current training set are detected by means of the same genetic algorithm used to identify the maximum uncertainty. The optimisation objective function is the minimum-square-error of the Rippa's estimator

$$E_{MSE-LOOCV}(\xi) = \frac{1}{N} \sum_{i=1}^N E_{Rippa,i}^2 \quad (10)$$

with $E_{Rippa,i}$ from equation (9).

It is worth noting that both the auxiliary and the stochastic hyperparameters have been optimised in a deterministic way, *i.e.*, through the standard RBF formulation. To inject uncertainty in the system, which is used to detect the next point to be added, the stochastic hyperparameter is varied in a range given by $\pm 15\%$ of the optimal value. The stochastic hyperparameters are sampled uniformly in their range, using a *Latin hypercube* sampling method to guarantee such a uniform distribution

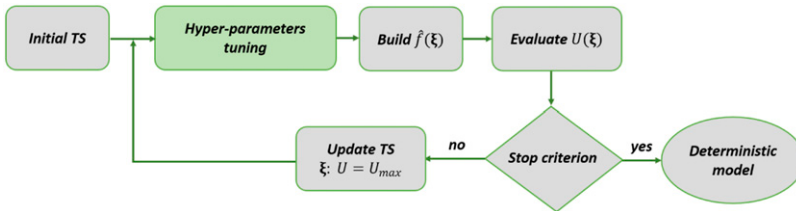


Figure 2. Flowchart of the dynamic adaptive metamodel update with kernel hyperparameter tuning.

with a number of samples that depends on the problem dimensionality so as to guarantee the statistic convergence.

Case study: Noise shielding

Existing aircraft noise prediction tools allow the computation of noise contours around airports as well as the noise certification levels, starting from aircraft tracks (in terms of altitude, speed, thrust and general configuration) and airport layout. From a broader viewpoint, a noise prediction tool can help the aircraft designer, and consequently the aviation industries, to drive markets towards increasingly eco-sustainable choices. In order to include innovative aircraft concepts within the well-assessed prediction tools, a feasible strategy could be providing a correction for the existing NPD (Noise-Power-Distance) curves, which represent a standard technique for evaluating the noise impact due to flight procedures. The NPD relationship provides noise levels as a function of observer distance via spherical spreading through a standard atmosphere, with suitable corrections to account for specific single-event metric (under standard meteorological conditions). Noise levels are integrated over the microphones array to yield a single value instead of instantaneous sound pressure level so as to represent the noise produced by infinite flight-paths with constant height and speed.⁵⁶ Corrections for innovative configurations deviating from what is considered in the NPD curves must be evaluated with computationally more expensive tools, *i.e.*, CAA numerical simulations. The method presented in the previous sections is used in the following to build a surrogate model of noise shielding for the application case of an airfoil in an uniform flow impinged by an incident field generated by a point source monopole, as depicted in Figure 3. The acoustic describer for the noise shielding effect characterisation is the Insertion Loss (IL), defined in frequency domain as it follows

$$IL = 20 \log_{10} \left(\frac{\tilde{p}_I}{\tilde{p}_T} \right) = SPL_I - SPL_T \quad (11)$$

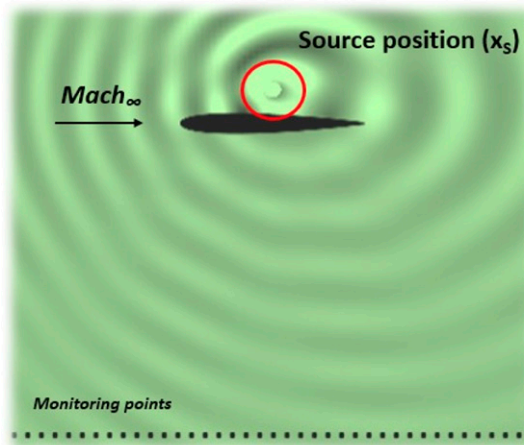


Figure 3. Total pressure field for an airfoil impinged by a point monopole source in the presence of a uniform flow. The insertion loss (IL) is evaluated at a linear array of virtual microphones (monitoring points).

where $\tilde{p}_T = \tilde{p}_I + \tilde{p}_S$ is the total pressure, \tilde{p}_I the incident pressure, \tilde{p}_S the scattered pressure and SPL is the sound pressure level ($\hat{\cdot}$ indicates Fourier transformation). Pressure data are computed using a boundary integral formulation for the solution of the convected Helmholtz equation, numerically solved with an in-house developed code implementing a zero-th order boundary element method (BEM) based on the collocation method. Specifically, we are interested in modelling the IL in one-third-octave bands integrated over a linear array of monitoring points, obtained by varying the flow speed and the source position. The independent variables domain is thus represented by the source location \mathbf{x}_s (above the lifting surface) and the Mach number \mathbf{x}_M . The design space bounds are $-0.5 < \mathbf{x}_s < 0.5$ (leading edge and trailing edge of the airfoil) and $0.1 < \mathbf{x}_M < 0.3$. An example of the resulting integrated IL fields for the one-third-octave band $f_c = 1250$ Hz is depicted in Figure 4.

Validation metric

Identifying relevant metrics to systematically validate and estimate the quality of metamodels is an essential aspect of this process, and it should be tailored to the application under analysis, namely, if we want to reach a global or local accuracy. Nevertheless, the stop criterion is also a crucial aspect, since in real applications the validation set (including the dynamically updated TS) can be non-representative of the global quality of the metamodel with areas of the design space unexplored. However, in this work, we present a benchmark application assuming the function is known densely to focus our attention on the proposed methodology. In adaptive surrogate-based analyses, another aspect to consider is the efficiency of reducing the number of necessary high-fidelity simulations required to obtain a reliable metamodel. Thus, the proposed kernels' aptitude is judged based on the final number of points added to reach the required accuracy (and consequently, the time and resources necessary to build the model). An evaluation criterion based on the metamodel uncertainty trend is inefficient for a kernel-based analysis with hyperparameter tuning. In fact, the uncertainty range is very sensitive to both the kernel and the stochastic range of hyperparameters variation (which, in this work, is updated at each iteration of the algorithm).

Therefore, a criterion based on the root-mean-square (RMS) error (%) between the validation set values and the metamodel prediction is used as a stop criterion (even though in actual applications, this issue must be further analysed due to the current validation set's representativeness). The normalised RMS error is computed as follows

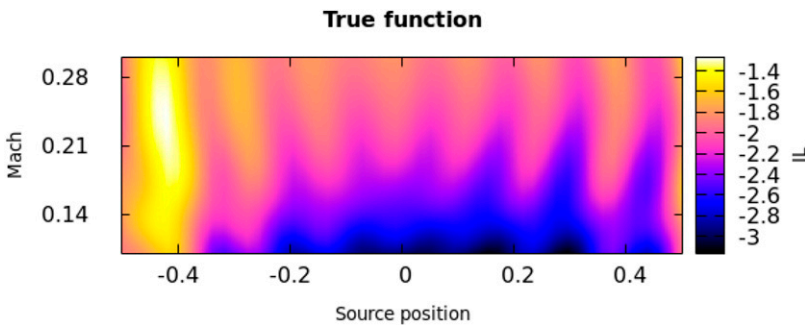


Figure 4. Integrated IL (frequency band $f_c = 1250$ Hz) for an airfoil geometry with unitary chord in presence of a uniform flow as function of source position (x axis) and Mach number (y axis).

$$E_{RMS}(\xi) = \sqrt{\frac{1}{N_{val}} \sum_{i=1}^{N_{val}} E(\xi_i)^2} \quad (12)$$

$$E(\xi_i) = \frac{|f(\xi_i) - \hat{f}(\xi_i)|}{\max(f) - \min(f)} \quad (13)$$

with ξ_i the i -th validation point. The RMS error has been selected because it is a global performance metrics, allowing to better compare the kernels in terms of position and number of points that must be added to guarantee a certain level of accuracy of the final metamodel.

Results

In this section, the results of the application of the proposed method to the case study described above are presented. For all the analyses, an initial TS of five points was set following the Central Composite Design⁵⁷ approach, and an uniform grid of 30×50 points was used as validation set. Figure 5 summarises the results obtained for all the third-octave bands in terms of points added (No. TS added) and maximum local relative error in percentage [%] obtained at the end of the iterative process (Max local Error). In the table, the kernels are indicated as PS (polynomial splines), GMQ (generalised multiquadric), TB (truncated Bessel) and GWP (Gaussian wave packet). As it can be seen in Figure 5, the GMQ and GWP kernels generally performs better than the other functions in terms of points added. Concerning the max. local error, GMQ presents the highest value at the lowest frequency ($f_c = 315\text{Hz}$). Observing all the frequencies, PS and TB kernels present the overall lower values of local errors for the target normalised RMS (set to the 3%), resulting thus the most robust kernel in terms of global accuracy. However, TB adds more points than the other functions, which is the reason for it presenting the lowest local errors especially for the highest frequency bands. Among the oscillatory kernels, GWP performed better than TB in terms of points added. In Figures 6–8, the metamodel prediction, the final TS , the local error (subfigs. (a), (b), (c) and (d)) and the RMS error trend (subfig. (e)) are shown for all the analysed kernels and for the frequency bands

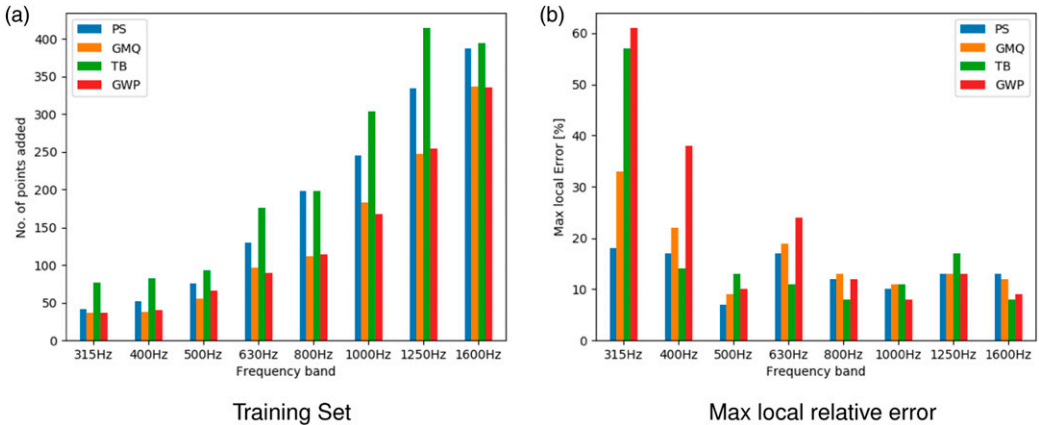


Figure 5. Noise shielding results: final number of points added to the training set (a) and maximum relative local error (b).

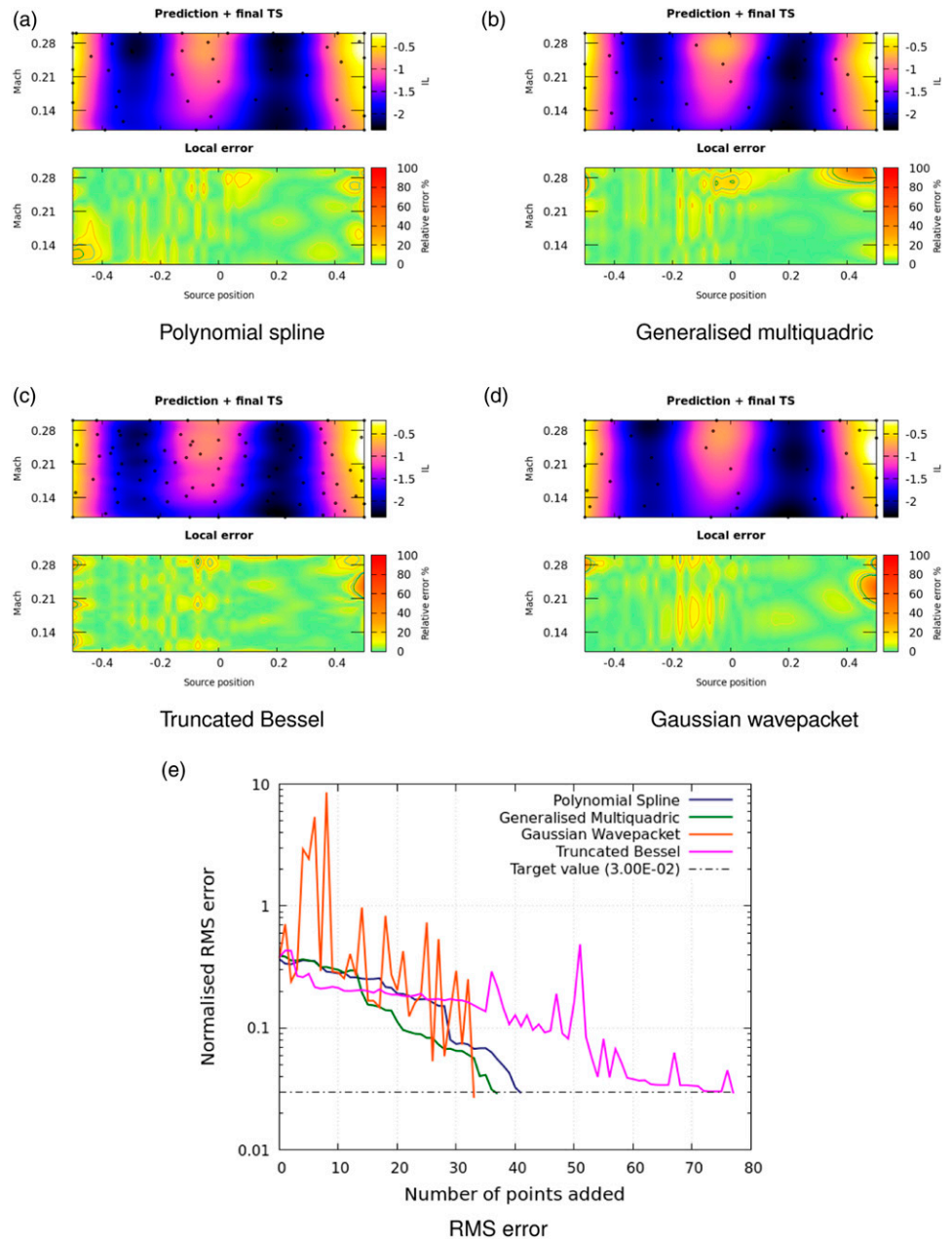


Figure 6. Integrated Insertion loss 2D, freq. band = 315 Hz.

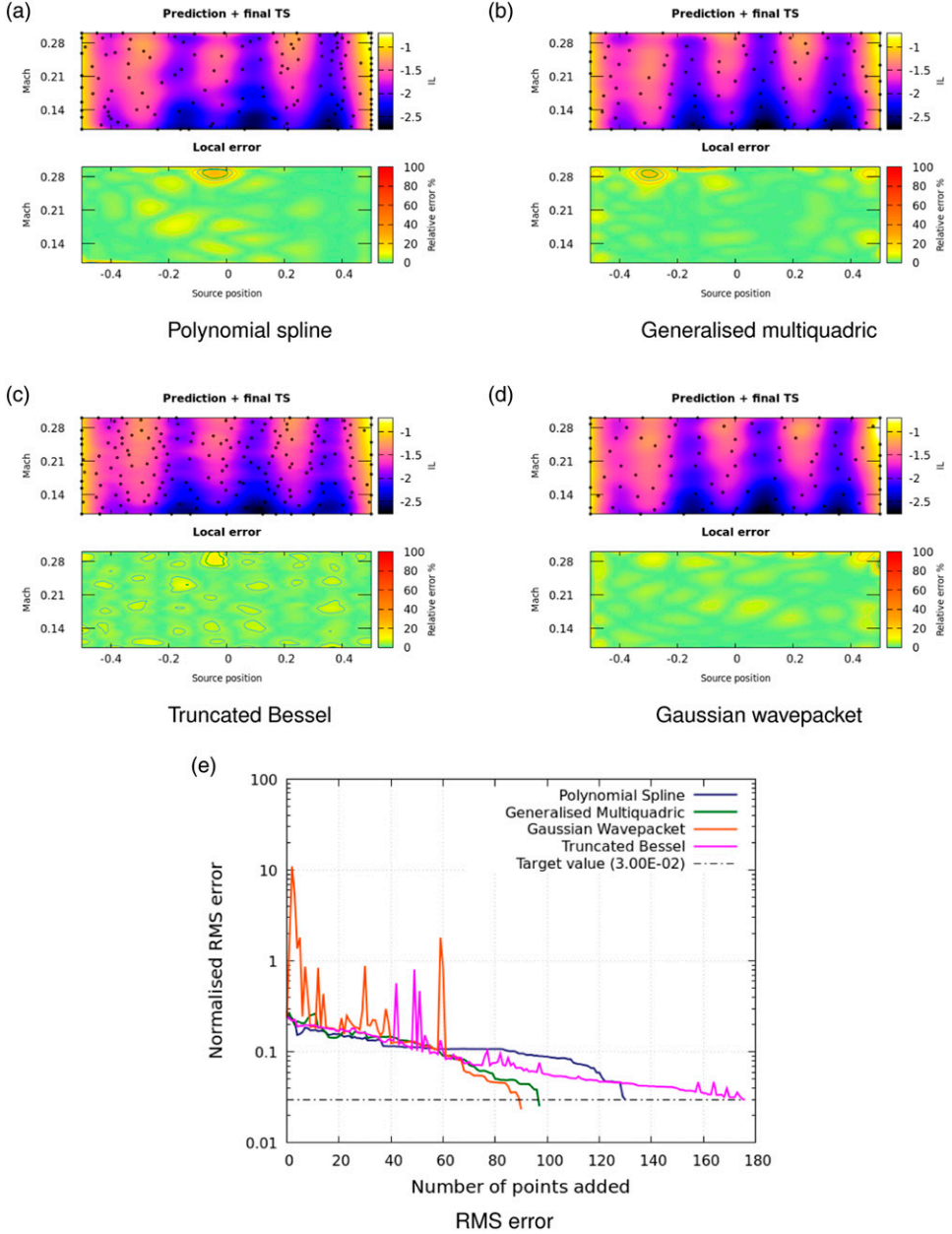


Figure 7. Integrated Insertion loss 2D, freq. band = 630 Hz.

$f_c = 315$ Hz, $f_c = 630$ Hz and $f_c = 1250$ Hz, respectively. Observing the RMS error trends for all the presented frequencies, GWP kernel (and similarly TB kernel, although at a lesser extent) presents several spikes, while PS and GMQ exhibit a much smoother behaviour.

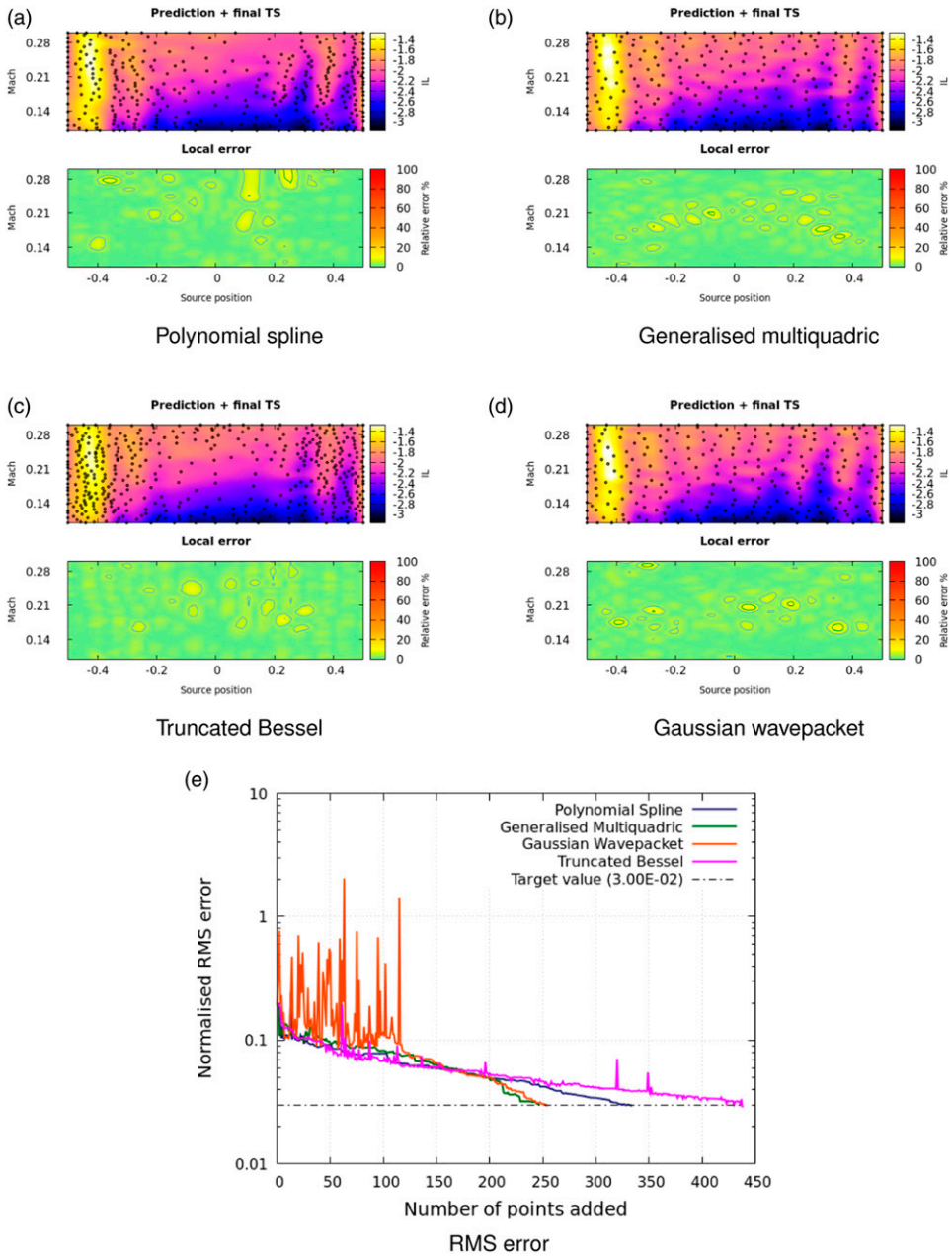


Figure 8. Integrated Insertion loss 2D, freq. band = 1250 Hz.

It should be noted that in real-life applications we cannot rely on the validation set to define a rule to exit the adaptive loop based on the RMS error between true function and prediction. As can be found in Volpi et al.,³⁰ the stop criterion is based on the metamodel uncertainty. The graph in Figure 9 shows the trend of the maximum uncertainty as a function of the number of points added to

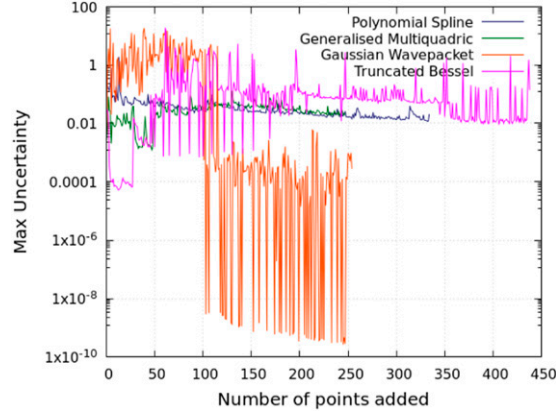


Figure 9. Trend of the maximum uncertainty for all analysed kernels (frequency band $f_c = 1250$).

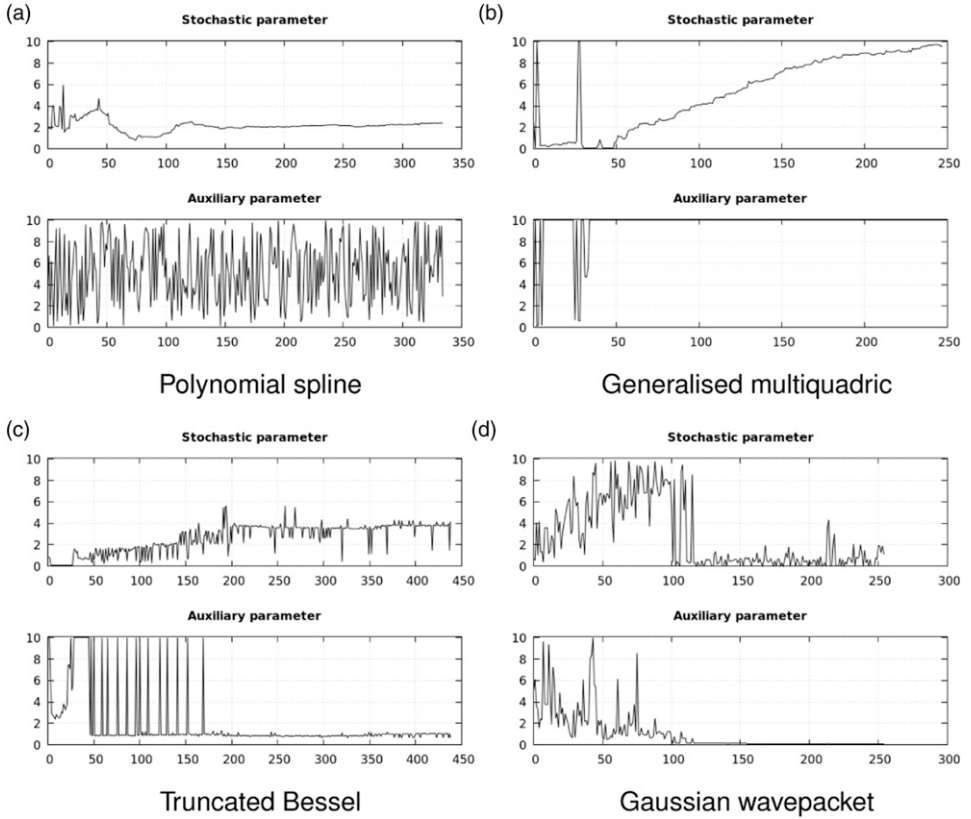


Figure 10. Optimal hyperparameter histories, freq. band = 1250 Hz.

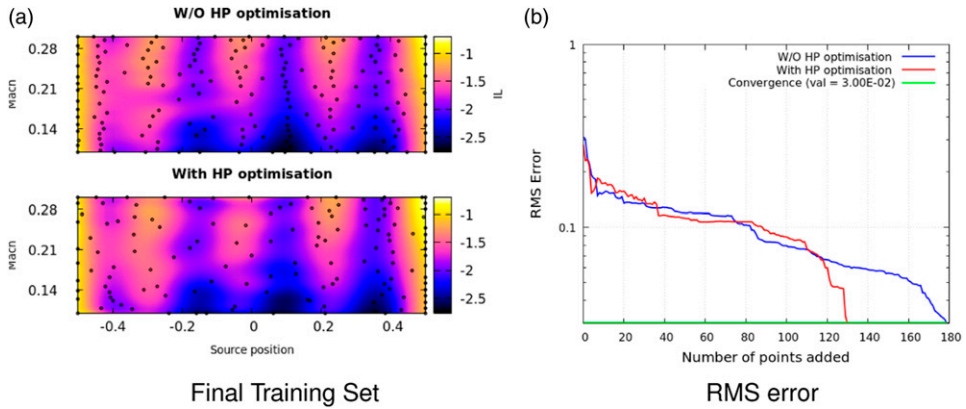


Figure 11. Comparison between metamodels with and without hyperparameter optimisation, freq. band = 630 Hz.

the TS in the adaptive loop for the frequency band $f_c = 1250$. A general noisy behaviour is observed, especially when the GWP and TB kernels are used. This behaviour turns out to be a side effect related to the way the stochastic metamodel is built. Indeed, the values of the metamodel uncertainty depend either on the kernel used (or on the auxiliary hyperparameter), and on the stochastic hyperparameter range which in turn depends on the optimal value of the stochastic parameter. On the other hand, the optimal values of the hyperparameters are strongly influenced by the characteristics of the TS (number of points and their distribution in the domain), which change at each iteration of the adaptive process, as can be observed in Figure 10. Therefore, it seems not possible to define a stop criterion based on the maximum uncertainty due to its severe fluctuations during the metamodel building, at least for the case of GWP and TB kernel functions. However, the PS and GMQ kernels appear to be more stable to such variations.

Nonetheless, the presented algorithm greatly helps in reducing the number of points needed to reach the required convergence, which is the most important feature in SBD for a given accuracy. A comparison between metamodels with and without hyperparameter optimisation is shown in Figure 11 for the frequency band $f_c = 630$ Hz. With respect to the adaptive scheme without hyperparameter tuning (shown in Figure 1), it has been noted that the tuning strategy helps to distribute the samples more uniformly, at least for the PS kernel.²¹ In fact, it is known³⁰ that polynomial splines basis tends to add new samples in regions where the function exhibits the maximum curvature, which can be a good characteristic if the metamodel is built within an optimisation framework but not if we want to explore the whole design space.

Conclusions

In this work, an adaptive metamodeling technique based on the *radial basis function* scattered data approximation method is proposed for aeroacoustic applications of innovative aircraft layouts. The method exploits the stochastic RBF formulation introduced by Volpi et al.³⁰ to evaluate the local metamodel uncertainty, which is used to drive the improvement of the training set with new samples in the more uncertain regions. A procedure to identify the optimal kernel hyperparameters is included at each iteration of the adaptive scheme to enhance the algorithm's performance and allow

to compare kernel functions for which a suitable range of hyperparameter values are difficult to be identified a priori in an adaptive approach where the training set varies at each iteration. To build the dynamic metamodel, the stochastic variable is sampled in a range defined as the $\pm 15\%$ of the optimal value, found by means of a suitable optimisation problem. The kernel hyperparameter tuning technique is based on the LOOCV method, where the Rippa estimator is used as operative research metric. The proposed technique has been applied to the case study of a simple airfoil in a uniform flow impinged by a point monopole source placed on top of the lifting surface. Specifically, the function to be reproduced is the Insertion Loss (*IL*) integrated over a linear array of receiver points, considering the Mach number and the point source position as design variables. An initial set of five training points based on the Central Composite Design sampling approach has been used to build a metamodel with the present technique, in which the exact value of *IL* has been obtained by solving the 2D convective Helmholtz equation through a BEM solver. The results are presented for several third-octave bands, showing that the method is able to successfully reproduce the Insertion Loss field with a given accuracy. Several kernel functions have been tested and compared to see how this design choice influences the adaptive metamodeling process. In particular, attention has been paid to the use of oscillatory and non-oscillatory kernels. It has been proved that using stochastic RBF, a reliable and accurate model of the *IL* noise shielding can be built using a limited number of direct simulations. This approach allows the designer to reduce the computational burden required to perform airport procedure and configuration optimisation of innovative aircraft configurations, for which the lack of historical data imposes the use of costly direct simulations in the design process. However, updating the stochastic range at each step of the adaptive loop leads to a noisy behaviour of the uncertainty trend, especially for the oscillatory kernels which have demonstrated to be particularly sensitive to the hyperparameters variation. Indeed, this issue is less severe for the polynomial spline and generalised multiquadric kernels, which are relatively stable bases for the RBF adaptive scheme. This issue represents a drawback of the proposed method since in real-life applications, where often it is not possible to rely on few validation points RMS error to establish the accuracy of the model, the uncertainty could be a good candidate to define the convergence of the method. Nevertheless, the proposed technique appears to be very promising for adaptive schemes, although further investigation is still necessary to identify a suitable metric for the stop criterion.

Declaration of conflicting interests


The author(s) declared no potential conflicts of interest with respect to the research, authorship, and/or publication of this article.

Funding

The author(s) disclosed receipt of the following financial support for the research, authorship, and/or publication of this article: This work has been supported by the European Union's Horizon 2020 research and innovation programme under project ANIMA (Aviation Noise Impact Management through novel Approaches) grant agreement No. 769627.

ORCID iDs

Lorenzo Burghignoli  <https://orcid.org/0000-0002-6410-0233>

Giorgio Palma  <https://orcid.org/0000-0003-4504-8123>

References

- Schlumberger CE. Air transport and energy efficiency (english). Transport papers, The World Bank, 2012. <http://documents.worldbank.org/curated/en/746271468184153529/Air-transport-and-energy-efficiency>.
- Forecast AGM. Growing horizons 2017/2036, 2017. ISBN: 978-2-9554382-2-6.
- IATA. Passenger demand. Technical report, International Air Transport Association, 2018. URL <http://www.iata.org/pressroom/pr/Pages/2018-05-03-01.aspx>.
- EC. Flightpath 2050, Europe's vision for aviation. Technical report, European Commission, 2011.
- Rizzi SA, Huff DL, Boyd DD et al. Urban air mobility noise: current practice, gaps, and recommendations (NASA/TP-2020-5007433). Technical Report October, NASA, 2020. <https://ntrs.nasa.gov/api/citations/20205007433/downloads/NASA-TP-2020-5007433.pdf>.
- ICAO. Environmental report 2016. Technical report, International Civil Aviation Organization, 2016. <https://www.icao.int/environmental-protection/Documents/ICAO%20Environmental%20Report%202016.pdf>.
- EAA and body or agency) EUASAE. European aviation environmental report 2019. Technical report, European Union, 2019. <https://ec.europa.eu/transport/sites/transport/files/2019-aviation-environmental-report.pdf>.
- EUH. Aviation noise impact management through novel approaches, 2020. <https://anima-project.eu/>.
- (FP7/2007-2013) ECSFP. Creating innovative air transport technologies for europe. <https://www.acare4europe.org/sites/acare4europe.org/files/document/Create-Final-Report-October-2010.pdf>.
- Palma G and Burghignoli L. On the integration of acoustic phase-gradient metasurfaces in aeronautics. *Int J Aeroacoustics* 2020; 19(6–8): 294–309. DOI: [10.1177/1475472X20954404](https://doi.org/10.1177/1475472X20954404).
- Palma G, Mao H, Burghignoli L, et al. Acoustic metamaterials in aeronautics. *Appl Sci* 2018; 8(6). DOI: [10.3390/app8060971](https://doi.org/10.3390/app8060971).
- Papamoschou D and Mayoral S. Jet noise shielding for advanced hybrid wing-body configuration. In 49th AIAA Aerospace Sciences Meeting including the New Horizons Forum and Aerospace Exposition. DOI: [10.2514/6.2011-912](https://doi.org/10.2514/6.2011-912).
- Czech MJ, Thomas R H and Elkoby R. Propulsion airframe aeroacoustic integration effects of a hybrid wing body aircraft configuration. *Int J Aeroacoustics* 2012; 11(3+4): 335–368.
- Qin N, Vavalle A, Le Moigne A et al. Aerodynamic considerations of blended wing body aircraft. *Prog Aerospace Sci* 2004; 40: 321–343. DOI: [10.1016/j.paerosci.2004.08.001](https://doi.org/10.1016/j.paerosci.2004.08.001).
- Clark L and Gerhold C. Inlet noise reduction by shielding for the blended-wing-body airplane. In 5th AIAA/CEAS Aeroacoustics Conference and Exhibit, Bellevue, WA, USA, 10–12 May 1999. <https://ntrs.nasa.gov/archive/nasa/casi.ntrs.nasa.gov/20040086845.pdf>.
- Research C and Service DI. ARTEM: Aircraft noise Reduction Technologies and related Environmental iMPact. https://cordis.europa.eu/project/rcn/212367_en.html.
- Centracchio F, Rossetti M and Iemma U. Approach to the weight estimation in the conceptual design of hybrid-electric-powered unconventional regional aircraft. *J Adv Transportation* 2018; 2018: 1–15. DOI: [10.1155/2018/6320197](https://doi.org/10.1155/2018/6320197).
- Beyer HG and Sendhoff B. Robust optimization – a comprehensive survey. *Computer Methods Appl Mech Eng* 2007; 196(33): 3190–3218. DOI: [10.1016/j.cma.2007.03.003](https://doi.org/10.1016/j.cma.2007.03.003).
- Zhou Q, Wang Y, Choi SK, et al. A sequential multi-fidelity metamodeling approach for data regression. *Knowledge-Based Syst* 2017; 134: 199–212. DOI: [10.1016/j.knosys.2017.07.033](https://doi.org/10.1016/j.knosys.2017.07.033).
- Wang GG and Shan S. Review of metamodeling techniques in support of engineering design optimization. *J Mech Des* 2007; 129(4): 370–380. DOI: [10.1115/1.2429697](https://doi.org/10.1115/1.2429697).
- Burghignoli L, Centracchio F, Iemma U, et al. Multi-objective optimization of a BWB aircraft for noise impact abatement. In: 25th International Congress on Sound and Vibration, ICSV25, Hiroshima, Japan:

- International Institute of Acoustics & Vibration, pp. 1256–1264. <http://www.proceedings.com/40638.html>.
22. Centracchio F, Burghignoli L, Rossetti M et al. Noise shielding models for the conceptual design of unconventional aircraft. In: 47th International Congress and Exposition on Noise Control Engineering, Inter-Noise 2018, Chicago, IL, USA: Institute of Noise Control Engineering, pp. 1677–1687. <http://www.proceedings.com/41633.html>.
 23. Wang C, Duan Q, Gong W, et al. An evaluation of adaptive surrogate modeling based optimization with two benchmark problems. *Environ Model Softw* 2014; 60: 167–179. DOI: [10.1016/j.envsoft.2014.05.026](https://doi.org/10.1016/j.envsoft.2014.05.026).
 24. Liu H, Ong YS and Cai J. A survey of adaptive sampling for global metamodeling in support of simulation-based complex engineering design. *Struct Multidisciplinary Optimization* 2018; 57(1): 393–416. DOI: [10.1007/s00158-017-1739-8](https://doi.org/10.1007/s00158-017-1739-8).
 25. Teixeira R, Nogal M and O'Connor A. Adaptive approaches in metamodel-based reliability analysis: A review. *Struct Saf* 2021; 89: 102019. DOI: [10.1016/j.strusafe.2020.102019](https://doi.org/10.1016/j.strusafe.2020.102019).
 26. Li G, Aute V and Azarm S. An accumulative error based adaptive design of experiments for offline metamodeling. *Struct Multidisciplinary Optimization* 2010; 40(1–6): 137–155. DOI: [10.1007/s00158-009-0395-z](https://doi.org/10.1007/s00158-009-0395-z).
 27. Martin J and Simpson T. Use of adaptive metamodeling for design optimization. In: 9th AIAA/ISSMO Symposium on Multidisciplinary Analysis and Optimization. Reston, Virginia: American Institute of Aeronautics and Astronautics, pp. 1–9. DOI: [10.2514/6.2002-5631](https://doi.org/10.2514/6.2002-5631).
 28. Diez M, Volpi S, Serani A, et al. *Simulation-based design optimization by sequential multi-criterion adaptive sampling and dynamic radial basis functions*. Springer International Publisher, Cham, 2019, pp. 213–228. DOI: [10.1007/978-3-319-89988-6_13](https://doi.org/10.1007/978-3-319-89988-6_13).
 29. Wang Q, Kim Y, Nafash J, et al. An adaptive augmented radial basis function-high-dimensional model representation method for structural engineering optimization. *Adv Struct Eng* 2020; 23(15): 3278–3294. DOI: [10.1177/1369433220931217](https://doi.org/10.1177/1369433220931217).
 30. Volpi S, Diez M, Gaul N, et al. Development and validation of a dynamic metamodel based on stochastic radial basis functions and uncertainty quantification. *Struct Multidisciplinary Optimization* 2015; 51(2): 347–368. DOI: [10.2514/3.13046](https://doi.org/10.2514/3.13046).
 31. Xiao NC, Zuo MJ and Zhou C. A new adaptive sequential sampling method to construct surrogate models for efficient reliability analysis. *Reliability Eng Syst Saf* 2018; 169(2006): 330–338. DOI: [10.1016/j.res.2017.09.008](https://doi.org/10.1016/j.res.2017.09.008).
 32. Hardy RL. Multiquadric equations of topography and other irregular surfaces. *J Geophys Res* (1896-1977) 1971; 76(8): 1905–1915. DOI: [10.1029/JB076i008p01905](https://doi.org/10.1029/JB076i008p01905).
 33. Buhmann MD. *Radial basis functions: theory and implementations*. Cambridge Monographs on Applied and Computational Mathematics, Cambridge University Press, Cambridge, UK, 2003. DOI: [10.1017/CBO9780511543241](https://doi.org/10.1017/CBO9780511543241).
 34. Schaback R. *A practical guide to radial basis functions*. <https://num.math.uni-goettingen.de/schaback/teaching/sc.pdf>. Electronic Resource, 2007.
 35. De Marchi S. Lectures on radial basis functions.
 36. Carroll D. Chemical laser modeling with genetic algorithms. *AIAA J* 1996; 34(2): 338–346. DOI: [10.2514/3.13069](https://doi.org/10.2514/3.13069).
 37. Zhao L, Choi KK and Lee I. Metamodeling method using dynamic kriging for design optimization. *AIAA J* 2011; 49(9): 2034–2046. DOI: [10.2514/1.J051017](https://doi.org/10.2514/1.J051017).
 38. Sasena MJ. *Flexibility and efficiency enhancements for constrained global design optimization with kriging approximations*. PhD Thesis, University of Michigan, 2002 <https://www.mat.univie.ac.at/~neum/glopt/mss/Sas02.pdf>.

39. Fornberg B, Larsson E and Wright G. A new class of oscillatory radial basis functions. *Comput Math Appl* 2006; 51(8): 1209–1222.
40. Lin J, Chen W and Sze KY. A new radial basis function for helmholtz problem. *Eng Anal Boundary Elem* 2012; 36(12): 1923–1930.
41. Londoño M and Montegranario H. Radial basis function-generated finite differences with bessel weights for the 2d helmholtz equation. *arXiv Cornell Univ* 2019.
42. Rashidinia J and Khasi M. Stable gaussian radial basis function method for solving helmholtz equations. *Comput Methods Differential Equations* 2019; 7(1): 138–151.
43. Fasshauer GE and Zhang JG. Multiquadric equations of topography and other irregular surfaces. *Numer Algorithms* 2007; 45(1): 345–368. DOI: [10.1007/s11075-007-9072-8](https://doi.org/10.1007/s11075-007-9072-8).
44. Schaback R. Error estimates and condition numbers for radial basis function interpolation. *Adv Comput Mathematics* 1995; 3(3): 251–264. DOI: [10.1007/BF02432002](https://doi.org/10.1007/BF02432002).
45. Fasshauer GE and Zhang JG. Preconditioning of radial basis function interpolation systems via accelerated iterated approximate moving least squares approximation. In Ferreira AJM, Kansa EJ, Fasshauer GE, et al. (eds.) *Progress on meshless methods*. Dordrecht: Springer, 2009. pp. 57–75. DOI: [10.1007/978-1-4020-8821-6_4](https://doi.org/10.1007/978-1-4020-8821-6_4).
46. Rippa S. An algorithm for selecting a good value for the parameter c in radial basis function interpolation. *Adv Comput Mathematics* 1999; 11: 193–210. DOI: [10.1023/A:1018975909870](https://doi.org/10.1023/A:1018975909870).
47. Roque C and Ferreira AJ. Numerical experiments on optimal shape parameters for radial basis functions. *Numer Methods Partial Differential Equations: An Int J* 2010; 26(3). DOI: [10.1002/num.20453](https://doi.org/10.1002/num.20453).
48. Mongillo M. Choosing Basis functions and shape parameters for radial basis function methods. *SIAM Undergraduate Res Online* 2011; 4: 190–209. DOI: [10.1137/11S010840](https://doi.org/10.1137/11S010840).
49. Kansa E and Carlson R. Improved accuracy of multiquadric interpolation using variable shape parameters. *Comput Mathematics Appl* 1992; 24(12): 99–120. DOI: [10.1016/0898-1221\(92\)90174-G](https://doi.org/10.1016/0898-1221(92)90174-G).
50. Fasshauer GE and Zhang JG. On choosing “optimal” shape parameters for RBF approximation. *Numer Algorithms* 2007; 45(1–4): 345–368. DOI: [10.1007/s11075-007-9072-8](https://doi.org/10.1007/s11075-007-9072-8).
51. Sarra SA and Sturgill D. A random variable shape parameter strategy for radial basis function approximation methods. *Eng Anal Boundary Elem* 2009; 33(11): 1239–1245. DOI: [10.1016/j.enganabound.2009.07.003](https://doi.org/10.1016/j.enganabound.2009.07.003).
52. Acar E. Optimizing the shape parameters of radial basis functions: an application to automobile crashworthiness. *Proc Inst Mech Eng Part D: J Automobile Eng* 2010; 224(12): 1541–1553. DOI: [10.1243/09544070JAUTO1560](https://doi.org/10.1243/09544070JAUTO1560).
53. Acar E and Rais-Rohani M. Ensemble of metamodels with optimized weight factors. *Struct Multidisciplinary Optimization* 2019; 37: 279–294. DOI: [10.1007/s00158-008-0230-y](https://doi.org/10.1007/s00158-008-0230-y).
54. Mullur AA and Messac A. Extended radial basis functions: more flexible and effective metamodeling. *AIAA J* 2005; 43(6): 1306–1315. DOI: [10.2514/1.11292](https://doi.org/10.2514/1.11292).
55. Zhou XJ, Ma YZ and Li XF. Ensemble of surrogates with recursive arithmetic average. *Struct Multidisciplinary Optimization* 2011; 44(5): 651–671. DOI: [10.1007/s00158-011-0655-6](https://doi.org/10.1007/s00158-011-0655-6).
56. Hullah P and Cavadini L. Aircraft noise modelling validation through the use of full 4-d flight trajectories including thrust calculation. In: 4th FAA-Eurocontrol R&D Conference, Santa Fe, New Mexico, 3-7 December 2001,
57. Box GEP and Wilson KB. On the experimental attainment of optimum conditions. *J R Stat Soc Ser B (Methodological)* 1951; 13(1): 1–45. <http://www.jstor.org/stable/2983966>.